DETERMINATION OF STRATUS CLOUDS OPTICAL PARAMETERS FROM AVHRR MEASUREMENTS

I.N. Melnikova,[1] I. Galindo,[2] and R. Solano[2]

[1]Center for Climate System Research, University of Tokyo,
[2]Centro Universitario de Investigaciones en Ciencias del Ambiente, Universidad de Colima,

Single scattering albedo and optical thickness of stratus clouds are obtained using asymptotic methods from AVHRR radiance measurements.

INTRODUCTION

Stratus clouds greatly impact the atmosphere energy balance and play an important role in weather or climate simulation, which may be explained, in turn, by their extension and high temporal stability, because the problem of studying the optical parameters of real stratus clouds became timely now. Satellite radiation measurements can be used for solving this.[1–3] But precedent studies were devoted for retrieval only of optical thickness assuming conservative scattering in cloud layer in the visual spectral range. Results obtained for clouds from airborne measurements show that it is not true in many cases in a real atmosphere.[4] The error of optical thickness retrieval without taking into account true absorption may be equal to 20% (Ref. 5).

In what follows we present an analytical method of interpretation of remote measurements of reflected radiance and irradiance[5,6] using AVHRR measurement data. The realization of the method is based on asymptotic formulas of radiative transfer theory representing a formal solution of the radiative transfer equation for a diffusive medium of high optical thickness (suitable for the case of stratiform cloudiness). The consideration is developed for a model of a horizontally infinite and homogeneous layer of large optical thickness.

OBSERVATIONAL DATA

Data used in this report are from our satellite ground receiving station located at the University of Colima campus at the city of Colima, Mexico. Images from the Advanced Very High Resolution Radiometer (AVHRR) channels 1 (0.58–0.68 μm) and 2 (0.725–1.10 μm) were calibrated using actual coefficients provided by NOAA. The percent albedo was converted to spectral radiance in physical units by procedures described in Refs. 7 and 8.

The processed data are from two consecutive satellite passes dated at 1996, day number 184 (July 2); the first is for NOAA–12 satellite at 13:38 GMT (7:38 local time) and the second for NOAA–14 at 21:03 GMT (15:03 local time). The geographical zone of both images is the same. It is located at 16°N, 103°W (SW of Mexico) and is sampled using a spatial resolution of 1.1 km per pixel Fig. 1a,b.

In order to have an idea about the visual aspect and geographical location, a GIF image was produced showing grid lines with an interval of 5′. The geo-referencing of each pixel in the images can be done with the aid of a grid of 14×14 ground control points, giving a total of 196 points with known coordinates. These points are numbered from 1 to 196 and are ordered from left to right and from top to bottom of the image. In the GIF image, they are marked with a red "+" sign. Additionally, for each ground control points the following parameters are given: the sun zenith angle, satellite zenith angle, sun-pixel-satellite angle and reflected sun-pixel-satellite angle. The images are expressed in units of radiance, $W/(m^2 \text{ micron sr})$ (Ref. 7). This was done following the appropriate calibration coefficients per each satellite. The numerical results of the radiance of calibrated images are exported into an ASCII file with the same dimensions (row, columns) as in the image. In order to find the percent of reflection function corresponding to these radiance values, one can invert the radiance calibrating formula, as stated in the following equation:

$$\rho(\mu_0, \mu) = I(\mu_0, \mu) \, 100 \, \pi W/(F\mu_0) \,, \qquad (1)$$

where $\rho(\mu_0, \mu)$ is the reflection function, $I(\mu_0, \mu)$ is the radiance value, in $W/(m^2 \text{ micron sr})$, W is the equivalent width of the spectral response function, in μm, of the AVHRR channels, and F is the integrated solar spectral irradiance, weighted by the spectral response function of the channel, in W/m^2.

Table I contains the values of W and F derived by NOAA (Ref. 7).

TABLE I. Values of W and F for AVHRR channels 1 and 2.

Satellite	$W1$	$F1$	$W2$	$F2$
NOAA–12	0.124	200.1	0.219	229.9
NOAA–14	0.136	221.42	0.245	252.29

The data in figure labelled 1841338 (Fig. 1a) correspond to NOAA–12 whereas directory 1842103 (Fig. 1b) corresponds to NOAA–14 polar orbiter.
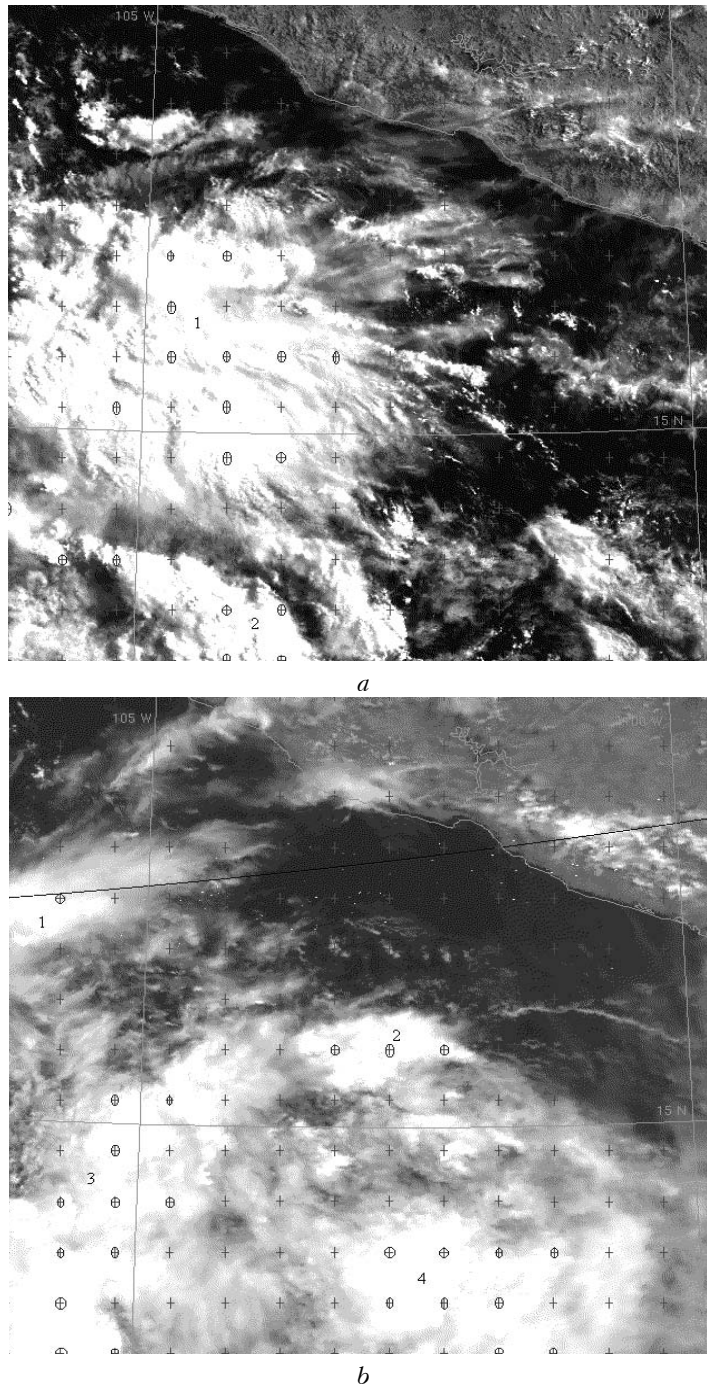
a

b

FIG. 1.   *Image for the first satellite flight: day number 184 (July 2, 1996): NOAA−12 at* 13:38 GMT *(*7:38 LT*) (a); NOAA−14 at* 21:03 GMT *(*15:03 LT*) (b).*

THEORETICAL BACKGROUND

It is known that reflected radiance in the units of incident solar flux for an optically thick layer with a weak true absorption is given by

$$\rho_{\infty}(\tau, \mu, \mu_0) = \rho_{\infty}(\mu, \mu_0) - \frac{m\bar{l}K(\mu)K(\mu_0)\exp(-2k\tau)}{1 - l\bar{l}\exp(-2k\tau)}, \quad (2)$$

where $\rho_{\infty}(\tau, \mu, \mu_0)$ is the reflection coefficient for a semi-infinite atmosphere; the function $K(\mu)$ describes the angular dependence of the radiance; the values m, l, k are constants determined by the scattering layer properties. In the case of small true absorption in comparison with scattering $(1 - \omega_0 \ll 1$, just the case of radiative transfer in the visible spectral region in clouds), these values are described by known expansions on powers of a small parameter $1 - \omega_0$,

Refs. 9 to 12. Here we use these expansions in terms of the parameter s where $s^2 = (1 - \omega_0)/[3(1 - g)]$ keeping the members with power equal 2.

$$k^2 = 3(1 - g)\,s\,;\quad m = 8\,s\,;\quad l = 1 - 6q'\,s + 18\,q'^2\,s^2\,;$$

$$K(\mu) = K_0(\mu)\,(1 - 3q's) + K_2(\mu)\,s^2\,; \tag{3}$$

$$\rho_\infty(\mu_0, \mu) = \rho_0(\mu_0, \mu) - 4K_0(\mu)\,K_0(\mu_0)\,s + \frac{a_2(\mu)\,a_2(\mu_0)}{12q'}\,s^2,$$

where $q' = 0.714$, $K_0(\mu)$ and $\rho_0(\mu_0, \mu)$ are the values of functions $K(\mu)$ and $\rho_\infty(\mu_0, \mu)$ with full absence of light absorption (conservative case, $\omega_0 = 1$). There are analytical expressions and table representations (Refs. 9 to 12) for $K_0(\mu)$, $\rho_0(\mu_0, \mu)$ and for the function $K_2(\mu)$ (Ref. 11). Thus there is the approximation for $K_0(\mu)$ with making use of exact calculations[13] as follows: $K_0(\mu) = 0.797\,\mu + 0.442$.

Analytical formulas (3) are derived mathematically quite strictly and their inaccuracy is determined by the terms $\sim s^3$, not accounted in these expansions. The following groups of formulas are approximations obtained in Refs. 5, 6, and 14 on the basis of the analysis of tabular values of functions $K(\mu)$, $a(\mu)$, and $\rho_\infty(\mu_0, \mu)$[9,13]:

$$K_2(\mu) = 5/3\,n_2\,(\mu^2 + 0.1)\,;$$

$$n_2 = 9\,q'^2 - 3(1 - g) + 2/(1 + g)\,;$$

$$a_2(\mu) = 3K_0(\mu)[3\,((1.271\mu - 0.9) + 4q')/(1 + g)]\,; \tag{4}$$

$$\rho_0(\mu, \mu_0) = (\mu + \mu_0)^{-1}\,[f_0(\mu)\,f_0(\mu_0) +$$

$$+ g(1.19\,\mu\mu_0 - 0.74(\mu + \mu_0) + 0.49)]\,,$$

where

$$f_0(\mu) = 0.937\,\mu + 0.529 \quad (\mu \geq 0.15)\,. \tag{5}$$

Let us suppose that the reflected radiance ρ_1 and ρ_2 are measured at two view angles μ_1 and μ_2, and for two different solar angles μ_{01} and μ_{02}. One can derive the expressions for s applying the first one from Eq. (2) for two pairs of angles μ_1, μ_2 and μ_{01}, μ_{02}, considering the ratio $(\rho_\infty(\mu_1, \mu_0) - \rho_1)/(\rho_\infty(\mu_2, \mu_0) - \rho_2)$ and putting the expansions (3) and relations (4), (5) as follows:

$$s^2 = \frac{[\rho_0(\mu_1, \mu_{01}) - \rho_1]\,K_0(\mu_2)\,K_0(\mu_{02})}{Dn} -$$

$$- \frac{[\rho_0(\mu_2, \mu_{02}) - \rho_2]\,K_0(\mu_1)\,K_0(\mu_{01})}{Dn}\,;$$

$$Dn = K_0(\mu_1)\,K_0(\mu_{01})\,[\rho_0(\mu_2, \mu_{02}) - \rho_2] \times$$

$$\times \left[\frac{K_2(\mu_{01})}{K_0(\mu_{01})} - \frac{K_2(\mu_{02})}{K_0(\mu_{02})} + 9q'^2\right] -$$

$$- K_0(\mu_2)\,K_0(\mu_{02})\,[\rho_0(\mu_1, \mu_{01}) - \rho_1] \times$$

$$\times \left[\frac{K_2(\mu_2)}{K_0(\mu_2)} - \frac{K_2(\mu_1)}{K_0(\mu_1)} + 9q'^2\right] +$$

$$+ \frac{K_0(\mu_1)\,K_0(\mu_{01})\,a_2(\mu_2)\,a_2(\mu_{02})}{12\,q'} -$$

$$- \frac{K_0(\mu_2)\,K_0(\mu_{02})\,a_2(\mu_1)\,a_2(\mu_{01})}{12\,q'}\,. \tag{6}$$

For optical thickness $\tau' = 3\tau(1 - g)$ the formula obtained in Ref. 14 is used

$$\tau' = (2s)^{-1}\,\ln\left\{\frac{m\,\bar{l}\,K(\mu_1)\,K(\mu_0)}{\rho_\infty(\mu_1, \mu_0) - \rho_1} + l\,\bar{l}\right\}\,. \tag{7}$$

These formulas contain only the measured values of ρ_1, ρ_2, and of the functions at fixed angles $\mu_{01,2}$, $\mu_{1,2}$, which may be found from the tables or from the above approximations, Eqs. (4) and (5). The value of the asymmetry factor (parameter g in Henyey-Greenstein phase function) is taken equal to 0.85. The detailed error analysis was accomplished earlier.[5,6] Uncertainties of the methodology increase for small optical thickness and large absorption. Thus it is good for thick clouds and visual light.

PARAMETERIZATION OF CLOUD HORIZONTAL INHOMOGENEITY

A simple approximate parameterization of the cloud top boarder inhomogeneity was suggested.[10] The geometrical variations at the top of the cloud layer increase the diffuse radiation of the incident flux. Hence it is essential for calculation of radiative characteristics depending on lighting conditions. Escape function and reflection function describes this dependence for reflected radiance and local albedo of semi-infinite medium − for irradiance. Then it is proposed to replace the functions of incident angle μ_0 by their modifications according to

$$\rho^*(\mu, \mu_0) = \rho^0(\mu, \mu_0)\,(1 - r) + ra(\mu)\,;$$

$$K(\mu_0) = K(\mu_0)\,(1 - r) + rn\,;$$

$$a(\mu_0) = a(\mu_0)\,(1 - r) + ra^\infty\,, \tag{8}$$

where spherical albedo a^∞, plane albedo $a(\mu_0)$, and value of n are defined as

$$a^\infty = 2\int_0^1 a(\mu_0)\,\mu_0\,d\mu_0 = 4\int_0^1 \mu_0\,d\mu_0 \int_0^1 \rho^0(\mu, \mu_0)\,\mu\,d\mu\,;$$

$$n = 2\int_0^1 K(\mu_0)\,\mu_0\,d\mu_0 \tag{9}$$

and the parameter r describes the completely diffuse part of light in the incident flux. In a similar manner the part of diffuse light within the incident flux may be taken into account.

It is useful to compare our results with recent more strict ones of cloud inhomogeneity impact on reflected radiation. There are many studies in this field last years.[15–18] In Ref. 15 it is shown that the influence of geometrical variations is larger than the internal one. The analytical solution of the problem made in Refs. 15 and 16 shows that cloud inhomogeneity impact on irradiance is actually described by replacement of the escape function by relations similar to Eqs. (8). There are many different evaluations of the power of such impact. In our case it is expressed by a value of parameter r. Analysis the above-mentioned studies allows to assume $r = 0.01$. Many results show also that the minimal disturbance in the radiation field is at solar angles for which $\cos \mu_0 \sim 0.6{-}0.7$. As it was mentioned earlier,[13] all functions, which are depending on incident angle, are approximately equal to the relevant integrals at these angles. Because we don't need the parameter r values if measurements are accomplished at suitable incident angles.

RESULTS OF RETRIEVAL

The present study concerns preliminary stage of satellite data processing. Thus, there are no detailed results pixel by pixel. Only data, which correspond to points marked by circles, were chosen for processing. There are several cloud fields in every picture. They are marked in Fig. 1 by figures.

Besides, we don't deal here with a detailed study of the horizontal inhomogeneity impact on uncertainties of methodology. This attempt revealed important questions, which will be answered, in further continuation of this work. As one can see, in Fig. 1 clouds are rather inhomogeneous in the horizontal plane especially in Fig. 1a. Besides, that solar elevation is not high, that's why the inhomogeneity is more effective in the first case. Thus at the first stage we obtain the optical thickness for every pixel assuming the independent pixel approximation and conservative scattering. Then for pixels with the same optical thickness for the same cloud field, single scattering albedo was retrieved by use of Eq. (6). It was not successful for all pairs of pixels. Processing of several pairs of pixels led to negative values for single scattering albedo, but use of other pairs of the same pixels give more realistic results. We assume that there is horizontal inhomogeneity only for optical thickness and constant absorption coefficient for every cloud field. Then the optical thickness is calculated by Eq. (7) for all pixels with single scattering albedo obtained for the cloud field considered. The obtained results are presented in Table II for the first and second satellite pass. Value of single scattering albedo showed only for pair of pixels where retrieval was successful.

TABLE II. *Radiation and geometric data and optical parameters retrieved for points processed.*

Pass number/Cloud field number	Point No.	μ_0	μ	I, W$^2 \cdot \mu$m$^{-1} \cdot$ sr^{-1}	$1 - \omega_0$	τ
1/1	74	0.2648	0.8335	182.77		6.0
1/1	75	0.2771	0.8840	167.08	0.0131	5.9
1/1	88	0.2596	0.8372	171.56	0.0131	5.5
1/1	102	0.2542	0.8409	154.54		4.8
1/1	103	0.2663	0.8904	242.15		14.5
1/1	104	0.2782	0.9339	219.18	0.0276	10.2
1/1	105	0.2899	0.9681	291.45	0.0285	25.5
1/1	115	0.2368	0.7928	286.97		35.6
1/1	117	0.2609	0.8936	259.52	0.0285	22.9
1/1	131	0.2555	0.8967	233.19		15.2
1/1	132	0.2673	0.9388	211.34	0.0276	11.4
1/2	156	0.2091	0.7547	283.77		80.3
1/2	157	0.2207	0.8048	286.97		81.0
1/2	173	0.2389	0.9060	219.74	0.0183	17.4
1/2	174	0.2505	0.9461	227.59	0.0183	17.9
1/2	187	0.2331	0.9092	183.89		9.9
1/2	188	0.2447	0.9485	193.41		10.9
2/1	57	0.8798	0.9548	161.24	0.061	3.2
2/1	58	0.8742	0.9184	144.8	0.061	2.9
2/2	105	0.8525	0.6778	174.81	0.180	1.6
2/2	106	0.8458	0.6312	169.1	0.101	1.2
2/2	107	0.8391	0.5877	161.24	0.101	1.0
2/3	115	0.8794	0.8634	153.73	0.036	2.6
2/3	116	0.8736	0.8172	164.09	0.024	2.4
2/3	129	0.8817	0.8602	166.6	0.050	2.7
2/3	141	0.8952	0.9392	127.65	0.023	2.8
2/3	142	0.8896	0.9005	148.37	0.042	2.8

Continuation of Table II

Pass number / Cloud field number	Point No.	μ_0	μ	I, $\text{W}^2 \cdot \mu\text{m}^{-1} \cdot \text{sr}^{-1}$	$1 - \omega_0$	τ
2/3	143	0.8839	0.8571	158.73	0.047	2.6
2/3	144	0.8780	0.8108	152.3	0.061	2.3
2/3	155	0.8971	0.9365	146.23	0.045	3.0
2/3	156	0.8915	0.8975	150.52	0.048	2.8
2/3	157	0.8859	0.8539	150.16	0.020	2.6
2/3	169	0.8989	0.9337	157.66	0.041	3.1
2/3	170	0.8934	0.8945	179.81	0.017	3.1
2/3	183	0.9006	0.9309	166.6	0.017	3.1
2/3	184	0.8951	0.8914	195.53	0.053	3.2
2/3	185	0.8894	0.8476	168.74	0.012	2.7
2/4	162	0.8546	0.6198	153.73	0.22	1.2
2/4	163	0.8478	0.5765	161.24	0.34	1.0
2/4	164	0.8407	0.5354	143.37	0.13	0.5
2/4	165	0.8335	0.4966	151.23	0.24	0.3
2/4	176	0.8564	0.6171	168.02	0.35	1.3
2/4	177	0.8495	0.5739	154.09	0.30	0.9
2/4	178	0.8424	0.5329	150.87	0.32	0.6
2/4	192	0.8441	0.5304	141.23	0.13	0.5
2/4	193	0.8368	0.4917	149.09	0.52	0.3

In some cases there was impossible to obtain optical thickness with use of formula (3). Then we applied formula for pure scattering condition, particularly for satellite pass 2 where clouds are thinner. So, errors of retrieval of optical thickness are big enough in some cases.

Relevant values of single scattering albedo and optical thickness are presented in Tables II. One can see that optical thickness is greater for the first picture especially for cloud field 1. In case of second satellite pass values of optical thickness are rather small, thus errors of the single scattering albedo retrieval are big.

Values of single scattering albedo are low for both pictures, so the true absorption in clouds considered is great. Results obtained are preliminary and it is supposed to process all cloud pixels in the pictures the same way. In the Fig. 1*b* (the second satellite pass) results appear to be more homogeneous as it is seen from Table II.

The proposed methodology is needed in detailed error analysis and taking into account the influence of different factors on the accuracy of this retrieval. The main questions which arise in this connection are: impact of cloud inhomogeneity; choice of the base pixel for scanning other pixels of the same cloud field paired with it and some other questions. But the possibility of obtaining optical parameters using a rather simple methodology looks optimistic.

REFERENCES

1. T.Y. Nakajima and T. Nakajima, J. Atmos. Sci. **52**, 4043–4059 (1995).
2. T. Nakajima and M.D. King, J. Atmos. Sci. **47**, 1878–1893 (1990).
3. A.N. Rublev, A.N. Trotsenko, and P.U. Romanov, Izv. RAS, Fiz. Atmos. Okeana **33**, No. 5, 670–675.
4. K.Ya. Kondratyev, V.I. Binenko, and I.N. Melnikova, Meteorology and Atmospheric Physics **65**, 1–10 (1997).
5. I.N. Melnikova, P.I. Domnin, V.V. Mikhailov, V.F. Radionov, J. Atmos. Sci. (in print).
6. I.N. Melnikova and P.I. Domnin, Atmos. Oceanic Opt. **10**, No. 7, 455–459 (1997).
7. H.B. Kidwell, (Comp. and Ed.), *NOAA Polar Orbiter Data. Users Guide* (National Oceanic and Atmospheric Administration, National Environmental Satellite, Data and Information Service, Washington, D.C., 1995).
8. L. Lauritsson, G.J. Nelson, and F.W. Porto, *Data Extraction and Calibration of TIROS-N/NOAA Radiometers,* NOAA Technical Memorandum NESS 107, Washington, D.C.
9. H.C. Van de Hulst, *Multiple Light Scattering. Tables, Formulas and Applications.* (Academic Press, 1980), Vols. 1 and 2, 739 pp.
10. V.V. Sobolev, *Light Scattering in Planet Atmospheres* (Nauka, 1972), 336 pp.
11. I.N. Minin, *Radiation Transfer Theory in Planetary Atmospheres* (Nauka, 1988), 264 pp.
12. E.G. Yanovitskij, *Light Scattering in Inhomogeneous Atmospheres* (Kiev, 1995), 400 pp.
13. I.N. Melnikova, Zh.M. Dlugach, T. Nakajima, and K. Kawamoto, Appl. Opt., J. Opt. Soc. Amer. (in print).
14. M.D. King, J. Atmos. Sci. **44**, No. 13. 1734–1751 (1987).
15. V.L. Galinsky and V. Ramanathan, J. Atmos. Sci. **55**, 2946–2955 (1998).
16. I.M. Tarabukhina, Izv. RAS, Fiz. Atmos. Okeana **23**, No. 2, 148–155 (1987).
17. G.A. Titov, J. Atmos. Sci. **55**, 1549–1560 (1998).
18. A. Marshak, A. Davis, W. Wiscomb, and R. Cahalan, J. Geophys. Res. **103**, No. D16, 19557–19567 (1998).